ITER-relevant transient heat loads on tungsten exposed to plasma and beryllium

2014 Phys. Scr. 2014 014036

(http://iopscience.iop.org/1402-4896/2014/T159/014036)

IOP Publishing | Royal Swedish Academy of Sciences Physica Scripta
Phys. Scr. **T159** (2014) 014036 (5pp) doi:10.1088/0031-8949/2014/T159/014036

ITER-relevant transient heat loads on tungsten exposed to plasma and beryllium

J H Yu[1], R P Doerner[1], T Dittmar[1], T Höschen[2], T Schwarz-Selinger[2] and M J Baldwin[1]

[1] Center for Energy Research, University of California at San Diego, La Jolla, CA 92093-0417, USA
[2] Max-Planck-Institut für Plasmaphysik (IPP), D-85748 Garching, Germany

E-mail: jyu@ferp.ucsd.edu

Received 16 May 2013
Accepted for publication 7 September 2013
Published 1 April 2014

Abstract
Tungsten (W) is presently the most attractive plasma facing material for future fusion reactors. Off-normal transient events such as edge localized modes and disruptions are simulated with a pulsed laser system in the PISCES-B facility, providing pulses with 1–10 ms duration with absorbed heat flux factors up to $\sim$90 MJ m^{-2} s$^{-1/2}$. This paper characterizes surface morphology changes and damage thresholds under transient heating on W exposed to He plasma or D plasma with and without Be coatings. W is damaged in the form of grain growth, surface roughening, melting and cracking. With a Be coating on the order of μm thick, the laser pulse produces a variety of Be surface changes including Be–W alloying, vaporization of the Be layer, melting and delamination.

Keywords: plasma, tungsten, beryllium, pulsed laser heating

(Some figures may appear in colour only in the online journal)

1. Introduction

Tungsten (W) is presently the most attractive plasma facing material for future fusion experiments such as ITER due to its low physical sputtering and performance at high temperatures. However, W will melt if exposed directly to large type I edge localized modes (ELMs), disruptions, or runaway electrons in future machines. In an effort to mitigate W damage due to thermal transients, an innovative approach was proposed to deposit sacrificial low-Z materials on W [1]. The idea behind this concept is that during transient heating the low-Z material would be vaporized and the heat load to the underlying W would be reduced. Here we extend previous studies of transient heat loads on W [2–6] and present preliminary work on pulsed laser heat loads on W with steady-state He or D plasma exposure, with and without Be seeding [7]. The Be layers used in the present study are $\leqslant 3\,\mu$m, which is thinner than required to significantly reduce ITER-relevant transient heat fluxes to the underlying W. However, laser irradiation of Be layers reveals rich morphology changes including complete layer removal, melting, cracking and delamination. Studying these transient heat-induced changes to Be layers could lead to insight into dust generation mechanisms in tokamaks.

2. Experimental set-up

An Nd:YAG laser with wavelength of 1064 nm is used to provide a controlled temperature rise by irradiating the surface of W samples (25.4 mm diameter and 2 mm thick) mounted on the sample manipulator in the PISCES-B linear plasma device. The laser pulse width can be varied from 1 to 10 ms, and the maximum peak power is 5 kW. The laser is guided by a set of turning mirrors over a distance of $\sim$20 m and a focusing lens is used to obtain the desired spot size at the target. Laser beamline losses are taken into account and 50% reflectivity of W [8, 9] at 1064 nm is used to estimate the absorbed laser power.

Standard rolled commercial grade polycrystalline W with purity $>$ 99.97% from Plansee was cut into discs using electric discharge machining. The as-received polycrystalline W had elongated grains with size 1–2 μm wide and 10–100 μm long. The orientation of the grains was parallel to the sample surface. Samples were surface ground with successively finer grades of abrasive from 220 to 1200 grit on a Struers TegraPol-11 grinding and polishing machine, and then polished with successively finer grades of polishing paste ranging from 9 to 1 μm. Samples were then ultra-sonically cleaned (but not outgassed) in acetone followed by ethanol.

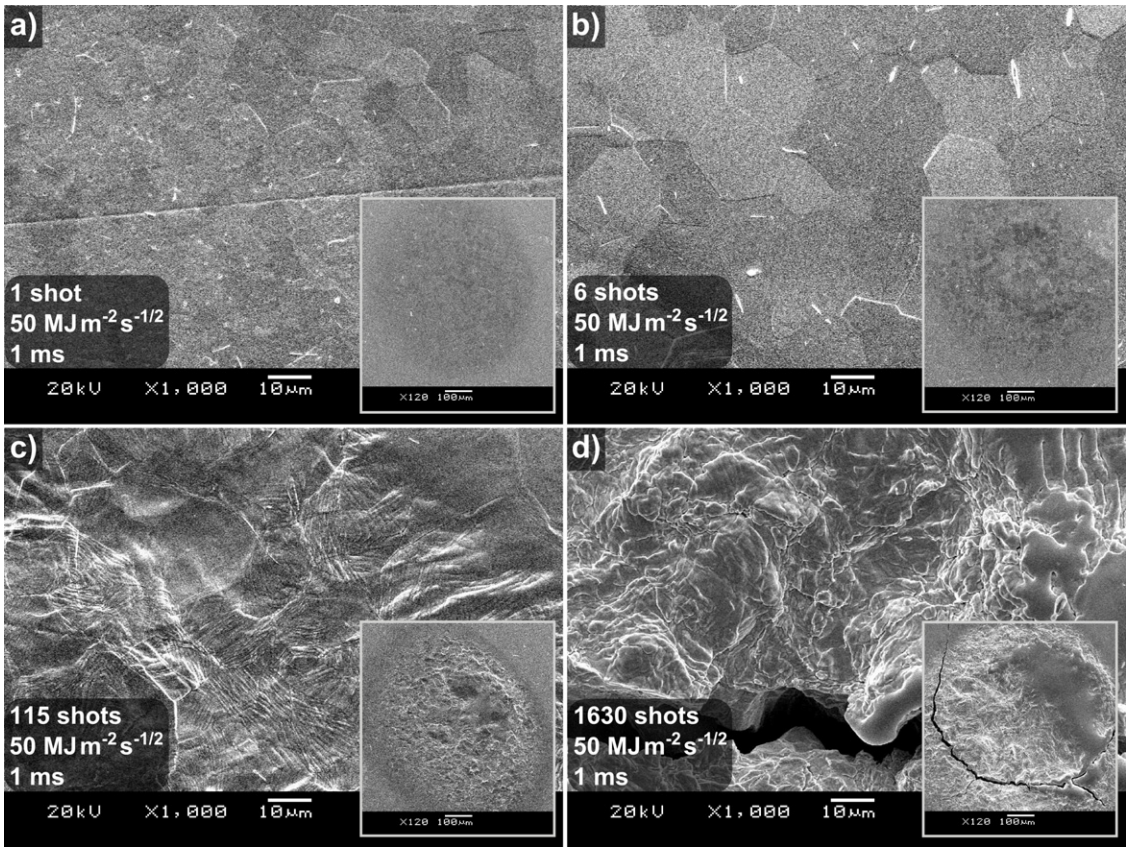

Figure 1. Absorbed laser power density of 1.6 GW m^{-2} and 1 ms pulse width during He plasma exposure. The number of laser shots and the He fluence at the start of the laser shots were (a) 1 shot, 1.4×10^{26} m^{-2}, (b) 6 shots, 4.5×10^{25} m^{-2}, (c) 115 shots, 1.5×10^{26} m^{-2} and (d) 1630 shots, 5.2×10^{25} m^{-2}. The inset figures show lower magnification views.

The laser irradiated W samples in the PISCES-B facility during and after plasma exposure with the following conditions: (i) W exposed to He plasma with plasma density $n_e = 5 \times 10^{18}$ m^{-3} and electron temperature $T_e \sim 8$ eV; (ii) W exposed to D plasmas with n_e ranging from 4 to 7×10^{18} m^{-3} and T_e ranging from 3 to 6 eV; and (iii) W exposed to D plasmas (similar plasma parameters as above) with Be seeding from an effusion oven with singly ionized Be concentration of 0.1–1% in the plasma. Ion energy to the sample was controlled with a bias voltage and ranged from approximately 30–70 eV. For reference, a bare W sample with no plasma exposure was also irradiated by the laser with various laser energy densities. The laser beam profile created a radial variation of surface temperature within the laser spot during the laser pulse. The full-width-half-maximum of the laser spot at the W target was 0.7–1.5 mm. All of the quoted heat flux factors in this paper correspond to the center of the laser spot where the energy density was largest. An aiming mirror was controlled remotely to allow the laser to irradiate multiple spots during a single plasma exposure. The steady-state temperature of the samples was measured by a thermocouple on the back of the actively cooled sample during plasma exposure and was below 55 °C for all data shown here. After laser exposure the samples were moved in air for analysis with a scanning electron microscope (SEM); a laser irradiated Be-coated sample was also analyzed using sputter x-ray photoelectron spectroscopy (XPS) to obtain depth profiles of atomic concentrations and 2 MeV ^{3}He nuclear reaction analysis (NRA) to measure the Be areal density.

3. Results

3.1. Transient heat loads on W with He plasma exposure

The formation of nanobubbles in W exposed to He plasma has been reported previously [10, 11] and there have been reports of nanobubbles decreasing the effective thermal conductivity near the surface by several orders of magnitude [12]. Here we build on previous studies and investigate the effect of He nanobubbles on the near-surface material response of W to thermal transients. In figure 1, SEM images of laser spots on a single W sample are shown for different numbers of laser pulses fired during He plasma exposure. Each laser pulse was identical with a 1 ms pulse width fired at 1 Hz repetition frequency, and the absorbed heat flux factor for each pulse was approximately 50 MJ m^{-2} $s^{-1/2}$. With a single laser shot, (a) small recrystallized grains can be seen on the surface and (b) the grains appear larger after six shots. (c) After 115 shots, the surface roughens and there are indications of melt flow as seen in the smooth region of the laser spot. (d) With 1630 laser shots, the roughening further increases and W experiences mechanical failure in the form of melting and large cracks due to thermal fatigue. Increased damage with number of

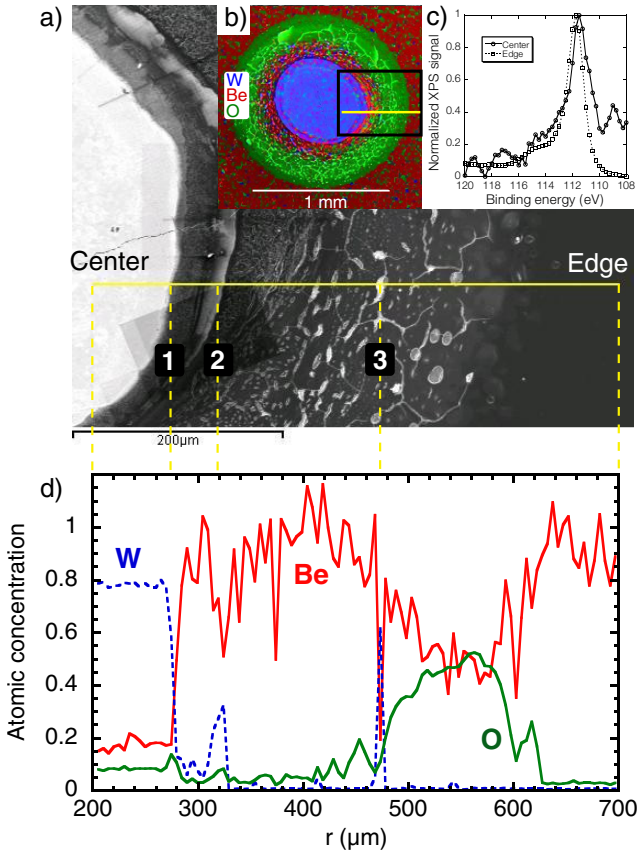

Figure 2. (a) SEM image of the damaged Be coating due to a single laser shot with estimated absorbed power density of 0.7 GW m^{-2} for 10 ms. The white areas show the underlying W where the Be coating was removed by the laser pulse. (b) Two-dimensional map of EDX analysis with W in blue, Be in red and O in green. The black rectangle shows the area of SEM image. (c) XPS spectra of the center of the spot (solid) and outside the spot (dashed), showing the shift between the Be1 s peaks for Be–W (111.4 eV) and Be (111.8 eV), respectively. (d) EDX line scan along the yellow lines in (a) and (b), showing the variation of W, Be and O concentrations due to the spatial variation in laser beam intensity.

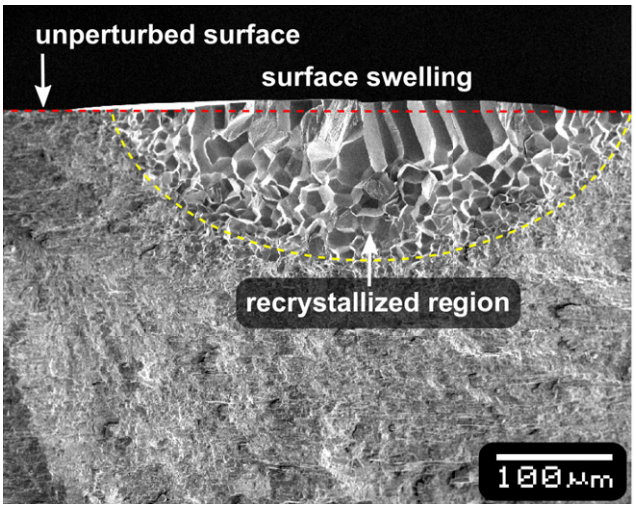

Figure 3. Ninety-degree cross section SEM image of a W sample broken after exposure to D plasma with Be seeding in the net erosion regime. Absorbed laser power density of 0.9 GW m^{-2} for 10 ms. The red dashed line shows the unperturbed surface and the yellow dashed line shows the approximate boundary of the recrystallized grain growth region.

thermal cycles has also been observed on W with electron beam thermal loading [2].

3.2. Transient heat loads on W exposed to D plasma with Be seeding

W samples were exposed to D plasma with Be seeding to investigate the transient heat load response of the mixed materials. For the case shown in figure 2 the sample was in the net deposition regime (ion energy ~50 eV), and a Be coating developed after a fluence of 1.2×10^{26} D m^{-2}. The Be layer was calculated to be 1.2 μm thick as determined by both sputter XPS depth profiling and NRA, and the thickness was measured to be approximately 3 μm from SEM imaging. The discrepancy between the thickness measurements may indicate that the Be layer was not fully compact, as the solid Be density was used in the XPS and NRA calculations.

Figure 2(a) shows an SEM image of part of the laser spot after a single shot, and figure 2(b) shows an energy dispersive x-ray (EDX) two-dimensional map of the surface elements over the entire laser spot. Figure 2(c) shows XPS spectra of the Be1S transition at two locations on the sample: (i) outside the laser spot where the Be coating remains intact (dashed line) and (ii) at the center of the spot where Be vaporization and Be–W alloying occurred (solid line). A shift is clearly visible between the two spectra, demonstrating the Be–W alloy formation. Figure 2(d) shows EDX line profiles of the atomic concentrations for W, Be and O along the horizontal solid yellow line in figure 2(a). The horizontal axis of figure 2(d) is aligned with the line scan of figure 2(a), and the dashed vertical yellow lines that are numbered show areas of interest. We use the Be signal in the location of the pure Be coating outside the laser affected area to normalize the Be concentration to 100%. The EDX Be atomic concentration near the center of the spot is 15–20%, which is in fairly good agreement with XPS sputter measurements that show Be at the 20% atomic concentration level due to Be–W alloy formation.

In the center region of the laser spot out to a radius of $r = 275\,\mu$m denoted by line 1, Be is vaporized and the underlying W is visible ($r = 0$ is the center of the spot). Moving further out from the center of the spot, the EDX Be signal increases dramatically. Moving to the location marked by line 2 in figure 2, the W signal increases in a small radial region, possibly because Be was only partially vaporized in this region. Beyond line 2, molten Be is formed between $r = 325$–$400\,\mu$m. At larger radii, the Be coating is cracked with holes that expose the underlying W. One such instance is seen by the spike in the W signal in figure 2(b) at line 3 at $r = 475\,\mu$m. Moving further away from the center of the laser spot, an annular region of oxygen is detected, and this oxygen signal is only seen on laser-flashed samples that had a Be coating (even on samples with Be coatings with estimated thickness < 10 nm). The physics behind the annular pattern of the oxygen signal is not completely understood. However, it is known that the formation of BeO is enhanced at high temperature above 750 °C [13], and we speculate that the oxygen EDX signal is from BeO that is formed as a result of increased surface temperature during laser heating.

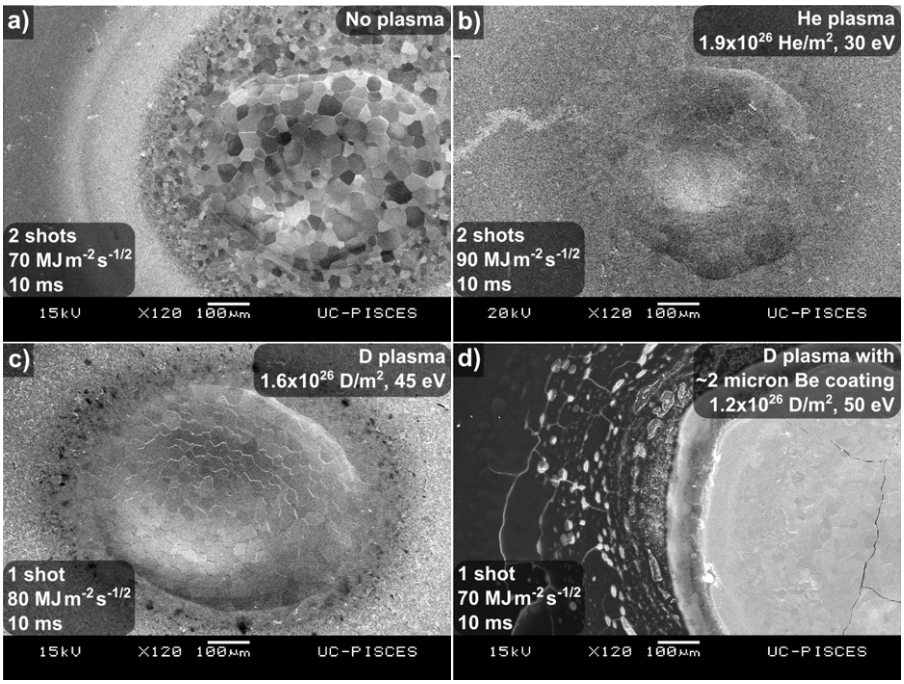

Figure 4. SEM images of laser induced damage on W with (a) no plasma exposure, (b) He plasma exposure, (c) D plasma exposure and (d) D plasma exposure with Be seeding forming a $\sim 2\,\mu$m thick Be layer.

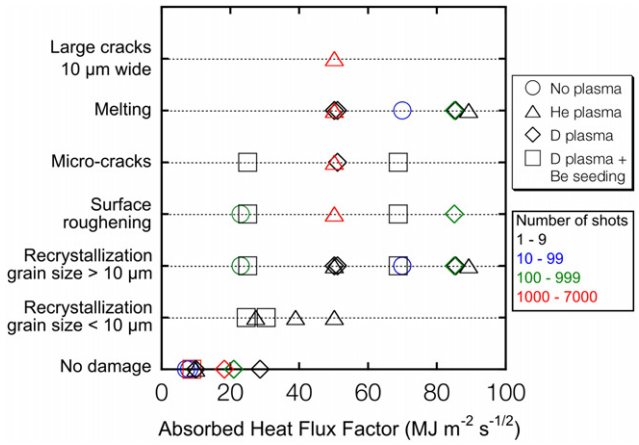

Figure 5. Laser-induced damage with 1–10 ms pulse widths for various plasma exposures as a function of absorbed heat flux factor. The number of laser shots is represented by the symbol color.

3.3. Comparison of W response to transient heat loads with various plasma exposures

The depth of the heat-affected zone is determined with SEM images of the cross-section of a W sample. In the case shown in figure 3 the W sample was exposed to D plasma with Be seeding, and a single laser shot was fired after the plasma was turned off. To image the cross section, the sample was intentionally broken along a groove (1 mm deep) that was cut in the back of the sample prior to plasma exposure. The laser was aimed on the front surface to align with the groove. The recrystallized region extends to a depth of over 100 μm with an approximate absorbed heat flux factor of 90 MJ m^{-2} s$^{-1/2}$. Figure 3 also shows that, along this particular cross section, the surface where the laser hits expands and swells upward by 10 μm relative to the unperturbed surface due to a volumetric increase of the W caused by thermal expansion and plastic deformation [2].

Figure 4 shows the response of (a) bare W, (b) He plasma-exposed W, (c) D plasma-exposed W and (d) D plasma-exposed W with Be seeding. The laser conditions were similar and recrystallized grain growth is seen in all cases. The SEM image of the laser shot on He-exposed plasma has evidence of an arc track, which has been observed on W in other linear devices after laser flashing during He plasma operation [6, 14]. Cracks appear in the underlying W with the Be layer, while no cracks appear on W without the Be layer for the same incoming laser energy densities. This difference is attributed to the formation of Be–W alloy which has a lower damage threshold compared to bulk W.

4. Discussion

A summary of the laser flashing experiments is shown in figure 5, where the vertical axis is a qualitative description of the W morphology changes due to transient laser heating. The absorbed heat flux factor is calculated at the center of the laser spot. It can be seen that the onset of W laser damage occurs at approximately 25 MJ m^{-2} s$^{-1/2}$ in the form of recrystallized grain growth and surface roughening. This threshold agrees (within the $\sim$30% uncertainty in the heat flux factor values) with that found by Linke *et al* [2], who observed the formation of a dense crack network at 20 MJ m^{-2} s$^{-1/2}$ on cool base temperature W exposed to 100 cycles of 120 keV electrons. Also seen in figure 5, W exposed to He plasma (red triangles) suffered the most damage presumably due to the presence of He nanobubbles, with thermal cycling at 50 MJ m^{-2} s$^{-1/2}$ causing melting and the formation of large cracks on the order of 10 μm wide. Multiple laser shots on D-exposed W (green diamonds) at 85 MJ m^{-2} s$^{-1/2}$ caused recrystallization,

surface roughening and a thin melt layer, but no cracking or gross melt flows. In the case of W exposed to D plasma with Be seeding (black squares), cracks appear in the central region of the laser spot where Be vaporization and Be–W alloy formation took place.

The deposition rate of eroded Be onto the ITER divertor is expected to be a maximum of $\sim$1 nm s^{-1} [15], implying that Be layers with thickness of order nm are expected to form between ELMs with expected frequency of $\sim$1 Hz. The Be sublimation energy density for such thin layers is negligible compared to the energy density from an off-normal event, so Be layers that naturally form in the ITER divertor will not provide protection to the underlying W.

5. Conclusion

Transient laser heating of W and Be-coated W during and immediately following D and He plasma exposure was performed in order to study structural changes and damage thresholds under off-normal events in future tokamaks. SEM images, EDX analysis and XPS spectroscopy show laser heating of Be-coated W creates rich morphology changes to the Be layer including complete layer removal, melting, cracking, delamination and Be–W alloy formation. The W surface expands up to 10 μm in response to a high heat flux factor of 90 MJ m^{-2} s$^{-1/2}$.

The onset of W damage induced by a 1064 nm laser occurs at approximately 25 MJ m^{-2} s$^{-1/2}$ in the form of recrystallized grain growth and surface roughening. At higher heat flux factors, melting and cracking occur, with the exact nature of the damage being influenced by the plasma exposure. More damage was observed for He-exposed W compared with D-exposed W. Future work includes repeating the laser flashing experiments at higher base temperature above the W ductile-to-brittle transition temperature.

References

[1] Wong C P C 2009 *J. Nucl. Mater.* **390** 1026
[2] Linke J *et al* 2011 *Nucl. Fusion* **51** 073017
[3] Loewenhoff Th *et al* 2011 *Phys. Scr.* **2011** 014057
[4] Morgan T W *et al* 2013 *J. Nucl. Mater.* **438** S96–101
[5] Thomser C *et al* 2011 *Phys. Scr.* **2011** 014059
[6] Umstadter K R *et al* 2011 *Nucl. Fusion* **51** 053014
[7] Doerner R P *et al* 2004 *Phys Scr.* **T111** 75
[8] Sakaguchi W *et al* 2009 *J. Nucl. Mater.* **390** 1149
[9] Yu J H *et al* 2013 *J. Nucl. Mater.* **438** S1150–4
[10] Yoshida N *et al* 2003 *Nucl. Fusion* **43** 655
[11] Iwakiri H *et al* 2000 *J. Nucl. Mater.* **283–287** 1134
[12] Kajita S *et al* 2007 *Nucl. Fusion* **47** 1358
[13] Aylmore D W *et al* 1960 *J. Nucl. Mater.* **2** 169
[14] Kajita S *et al* 2013 *Nucl. Fusion* **53** 053013
[15] Schmid K 2008 *Nucl. Fusion* **48** 105004